

lation, **1** was fully acylated after a 24-h incubation with trifluoroethyl esters of both longer aliphatic (octanoic, myristic, and palmitic) and aromatic (phenylacetic) acids. Analysis of the products<sup>10</sup> revealed that in all cases only *N*- $\epsilon$ -monoacyl-**1** compounds were formed.

In order to explain the striking  $\epsilon$ -specificity of lipase with **1**, we examined the acetylation of several other peptides in acetonitrile. It was found that L-Ala- $\alpha$ -L-Lys-O-*t*-Bu had essentially the same reactivity as **1** and the product of the enzymatic reaction was the *N*- $\epsilon$ -monoacetyl dipeptide. Hence the phenyl ring in **1** is not responsible for the low reactivity of the  $\alpha$ -NH<sub>2</sub> group compared to  $\epsilon$ . However, the reactivity of the  $\alpha$ -NH<sub>2</sub> group in L-Phe-NH<sub>2</sub> was (i) just 3 times lower than that of the  $\epsilon$ -NH<sub>2</sub> group in **1**, but (ii) 180 times greater than that of the  $\alpha$ -NH<sub>2</sub> group in L-Phe-O-*t*-Bu. These data suggest that the lipase is intolerant of a bulky main (but not side) chain of the peptide. This factor, however, plays no role in the reactivity of the  $\epsilon$ -NH<sub>2</sub> group (presumably due to its remoteness from the main chain), for the rates of enzymatic acetylation of **1** and of the smaller *N*- $\alpha$ -acetyl-L-Lys-NHCH<sub>3</sub> were identical.

Lipase was also found to selectively esterify Ser in a peptide. In fact, the acylation of Ser in the model peptide L-Phe-L-Ser-NH- $\beta$ -Naph (**2**) was even faster than that of Lys in **1**: the enzymatic conversions in *tert*-amyl alcohol (the former peptide is insoluble in acetonitrile) after 1.5 h were 98% and 52%, respectively. The NMR analysis<sup>10</sup> of the product revealed it to be exclusively *O*-monoacetyl-**2**, thus pointing to lipase's overwhelming preference for Ser's OH vs (chemically more reactive) Phe's NH<sub>2</sub> group.<sup>12</sup> The same result was obtained in the preparative enzymatic palmitoylation of the dipeptide.<sup>12</sup> In contrast, chemical acetylation with equimolar acetic anhydride yielded approximately 50% of the *N,O*-diacetyl-**2**, with the rest being the unreacted dipeptide.

In closing, we have developed a facile methodology for regio- and chemoselective enzymatic incorporation of various acyl moieties into short peptides. We are currently exploring its extension to longer peptides and to proteins.

(12) Thus allowing for the direct acylation of a hydroxyl group without protecting an amino group first.

(13) This work was financially supported by NIH Grant GM39794. L.S. is grateful to the Research Area of Trieste (Trieste, Italy) for a fellowship. We thank Hiroshi Kitaguchi for his help in peptide synthesis.

## Solid-State Photochemical Generation of A Very Stable Phenoxy-Phenoxy Radical Pair

David A. Modarelli and Paul M. Lahti\*

Lederle Graduate Research Tower  
Department of Chemistry, University of Massachusetts  
Amherst, Massachusetts 01003

Clifford George

Code 6030, Naval Research Laboratory  
Washington, D.C. 20375

Received February 20, 1991  
Revised Manuscript Received June 6, 1991

We have recently reported our finding that aryl oxalate derivatives are convenient, effective unimolecular photochemical sources of aryloxy radicals.<sup>1-3</sup> As a result, it is now possible to

explore aspects of aryloxy radical chemistry that were not easily probed by the standard solution bimolecular methods for generating such radicals.<sup>4</sup> In this paper we report the generation, electron spin resonance (ESR) observation, and thermal stability of remarkably persistent phenoxy-phenoxyl  $\pi$ -radical pairs generated by polycrystalline solid-state photolysis of bis(2,6-di-*tert*-butyl-4-methoxyphenyl) oxalate.

Generation and direct cryogenic observation of radical pairs trapped in proximity in the solid state is a well-established phenomenon.<sup>5</sup> However, radical pairs typically recombine or react upon warming, and are not readily kept at room temperature. In a case closely related to our work, McRae and Symons<sup>6</sup> found that 77 K solid-state  $\gamma$  radiolysis (but not UV-vis photolysis) of diaryl carbonates produced both isolated and triplet-paired phenoxy radicals, which disappeared on warming.

We found upon quartz-filtered xenon-arc UV-vis photolysis<sup>7</sup> of a powder sample of bis(2,6-di-*tert*-butyl-4-methoxyphenyl) oxalate **1** at 77 K under vacuum for ca. 3 min, the production of a reddish sample having a strong central ESR peak<sup>8</sup> with  $g = 2.0051$ , attributable to isolated 2,6-di-*tert*-butyl-4-methoxyphenyl radical (2,6-Bu-4-OMe-Phen). In addition, we were able clearly to observe six peaks consistent with the pattern expected for a randomly oriented triplet sample having zero-field-splitting (zfs) parameters  $|D'| = 116$  G,  $|E'| = 6.0$  G, with  $g_{xx} = 2.0060$ ,  $g_{yy} = 2.0057$ , and  $g_{zz} = 2.0040$ . The presence of a  $\Delta M_s = 2$  transition in the  $g = 4$  region confirms the presence of a triplet state species, which we attribute to interaction of a geminate pair of 2,6-Bu-4-OMe-Phen radicals, constrained in the crystal matrix of the precursor diaryl oxalate (DAO) after double decarbonylation (Scheme I).

The line shape of the triplet ESR spectrum was simulated by the method of Kottis and Levebvre<sup>9,10</sup> based upon the above values and is shown as curve b of Figure 1. The reddish color and  $g$  values are consistent<sup>11</sup> with generation of 2,6-Bu-4-OMe-Phen radicals. After the sample was annealed to room temperature and recooled, spectrum a (Figure 1) changed and a new radical-pair spectrum became evident. An example of the new spectrum obtained without a contaminating component of spectrum a is shown in Figure 1 as spectrum c, characterized by zfs parameters  $|D'| = 133$  G,  $|E'| = 6.7$  G, with  $g_{xx} = 2.0060$ ,  $g_{yy} = 2.0056$ , and  $g_{zz} = 2.0044$  (see simulated curve d). We attribute spectrum a to an initially formed geminate radical pair after photolysis that upon annealing reorganizes to a more stable geometric arrangement in the crystal to give spectrum c, which remains stable for days at room temperature under vacuum. The

(3) Modarelli, D. A.; Lahti, P. M. *J. Chem. Soc., Chem. Commun.* **1990**, 1167.

(4) (a) Solution oxidation methods are well described in: Mueller, E.; Mayer, R.; Narr, B.; Schick, A.; Scheffler, K. *Justus Liebigs Ann. Chem.* **1961**, 645, 1 and papers following in that issue. (b) An example of a photochemically based bimolecular oxidation method is described in: Griller, D.; Ingold, K. U.; Scaiano, J. C. *J. Magn. Reson.* **1980**, 38, 169. (c) A unimolecular photochemical method for phenoxy radical generation based upon bis(cyclohexadienone) peroxides has been described in: Cook, C. D.; Fraser, M. *J. Org. Chem.* **1964**, 29, 3716.

(5) Compare for instance the discussions and citations in the excellent studies of dibenzoyl peroxide solid-state photolysis: Vary, M. W.; McBride, J. M. *Mol. Cryst. Liq. Cryst.* **1979**, 52, 133; McBride, J. M.; Vary, M. W. *Tetrahedron* **1982**, 38, 765.

(6) McRae, J. A.; Symons, M. C. R. *J. Chem. Soc. B* **1968**, 428. The zfs values observed for this phenoxy-phenoxyl pair were  $|D'| = 144$  G,  $|E'| \approx 0$  G.

(7) On the basis of a typical maximum extinction coefficient of  $\epsilon \approx 2000$  M<sup>-1</sup> cm<sup>-1</sup> in these DAO's at ca. 270 nm, for the crystal density of 1.066 g/cm<sup>3</sup> for DAO **2**, the irradiating light should penetrate to a distance of ca. 25  $\mu$ m; hence, unfiltered photolysis mostly occurs on the surfaces of these solid samples.

(8) All  $g$  values in this article were determined relative to solid external diphenylpicrylhydrazyl radical standard with  $g = 2.0037$ . (Wertz, J. E.; Bolton, J. R. *Electron Spin Resonance: Elementary Theory and Practical Applications*; Chapman and Hall: New York, 1986; p 238 ff.)

(9) Kottis, P.; Levebvre, R. *J. Chem. Phys.* **1963**, 39, 393.

(10) Kottis, P.; Levebvre, R. *J. Chem. Phys.* **1964**, 41, 379.

(11) A good review of the stabilized phenoxy radicals—including some ESR and UV-vis spectral data—is given in Altwickler, E. R. *Chem. Rev.* **1967**, 67, 475.

(1) Modarelli, D. A.; Rossitto, F. C.; Lahti, P. M. *Tetrahedron Lett.* **1989**, 4473, 4477.

(2) Modarelli, D. A.; Rossitto, F. C.; Minato, M.; Lahti, P. M. *Mater. Res. Soc. Symp. Proc.* **1990**, 173, 83.

## Scheme 1

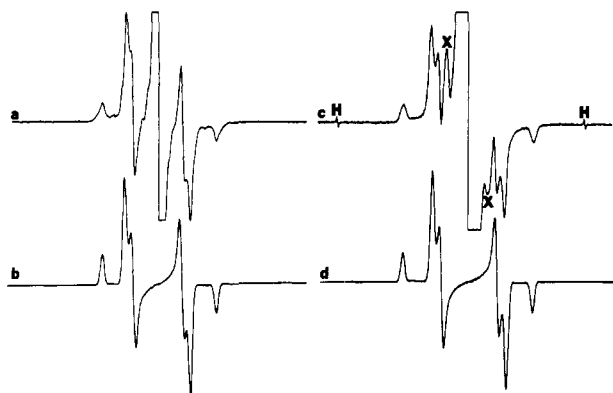
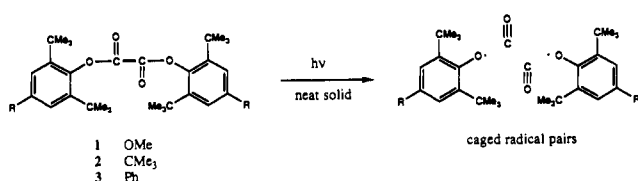


**Figure 1.** (a) ESR spectrum from brief photolysis of **1**, before annealing. (b) Random triplet simulation, using  $|D'| = 116$  G,  $|E'| = 6.0$  G, with  $g_{xx} = 2.0060$ ,  $g_{yy} = 2.0057$ , and  $g_{zz} = 2.0040$ . (c) ESR spectrum from photolysis of **1**, without contamination by spectrum a. The peaks marked with "X" are due to a presently unidentified signal carrier<sup>21</sup> that is usually observed under these conditions. The peaks marked "H" are due to hydrogen atoms. (d) Random triplet simulation, using  $|D'| = 133$  G,  $|E'| = 6.7$  G, with  $g_{xx} = 2.0060$ ,  $g_{yy} = 2.0056$ , and  $g_{zz} = 2.0044$ . All spectra are plotted from 3110–3710 G at spectrometer frequency 9.6 GHz.

nature of the geometric reorganization is not clear from our present data, but cannot be extreme<sup>12</sup> given the similarity of spectra a and c.

Although the thermal stability of the triplet radical pair from **1** is remarkable by comparison to other literature examples, it is understandable given the known stability of 2,6-di-*tert*-butyl-4-substituted phenoxy radicals<sup>11</sup> and the rigidity of the crystalline phase<sup>13</sup> in trapping geminate pairs of molecules and molecular fragments. We have not yet obtained single crystals of DAO **1** due to its thermal instability to room temperature crystallization and its tendency to form microcrystalline powders at lower temperatures, but X-ray crystal structures of similar DAO's **2** and **3** show both to have *s*-trans conformations with similar geometries of the phenoxy fragments. If **1**–**3** have similar structures and we assume that interacting phenoxy fragments in the radical pairs do not move relative to the precursor positions, we can estimate their zfs parameters by the spin-dipolar<sup>14</sup> ESR Hamiltonian, using a model described by McWeeny,<sup>15</sup> which has been converted to

(12) The crystal structure distance between ester oxygens for **2** is only 3.7 Å. But, by a purely dipolar model<sup>6</sup> in triplet spectrum a the effective inter-electronic distance is 6.2 Å, for spectrum c 6.0 Å, with the difference due qualitatively to delocalization of spin density in the component phenoxy radicals and perhaps partially to movement apart of radical fragments from the precursor positions.

(13) For a useful reference describing photochemistry in the crystalline phase, see: Cohen, M. D. *Angew Chem., Int. Ed. Engl.* **1975**, *14*, 386 and citations therein.

(14) Spin-orbit coupling was invoked by McBride and Vary<sup>5</sup> to explain their radical-pair spectra, since their zfs parameters could not be simulated by a structurally reasonable spin-density distribution interacting in a purely dipolar fashion. While some component of spin-orbit coupling may contribute to the zfs in our radical pairs, we can simulate our zfs parameters to fairly good accuracy by use of only the dipolar portion of the spin Hamiltonian and the geometric model described in the text (see also supplementary material). Given present uncertainty as to precise radical geometric placements and spin distributions in our polycrystalline DAO samples, attempts to quantitate spin-orbit coupling would seem to be rendered imprecise at this time.

(15) McWeeny, R. *J. Chem. Phys.* **1961**, *34*, 399.

a computer program ZFS described<sup>16</sup> and used<sup>17</sup> elsewhere. We modeled interacting phenoxy radicals assumed to have the experimental spin-density distribution<sup>18</sup> of 2,4,6-tri-*tert*-butylphenoxy (2,4,6-Bu-Phen) and found  $|D'| = 139$  G with  $|E'| = 1.1$  G, in reasonable agreement<sup>19</sup> with the observed zfs values for the triplet pairs from **1**. Some variation in  $|D'|$  predictions might be caused by differences in spin-density distribution between 2,6-Bu-4-OMe-Phen and 2,4,6-Bu-Phen, but we find by INDO level<sup>20</sup> computations that the spin density in the ipso C=O region of the radicals is not greatly changed by 4-methoxy substitution vs 4-alkyl substitution. Since the greatest effect upon the computed  $|D'|$  values is caused by variation in spin density of the proximate ipso regions of the radical pairs, the INDO results support assumption of similar spin densities in Bu-4-OMe-Phen and 2,4,6-Bu-Phen as a reasonable—though by no means unambiguously usable—model.

As additional support for this picture, we observed from 77 K photolysis of polycrystalline DAO **2** (along with a monoradical peak) a weak triplet radical-pair spectrum that persists for days under vacuum at 25 °C, with zfs parameters of  $|D'| = 106$  G,  $|E'| = 5.5$  G, and a  $\Delta M_s = 2$  transition in the  $g = 4$  region. This spectrum is complicated by additional lines that we have not yet assigned, but it appears that a geminate 2,4,6-Bu-Phen radical pair is produced, with a  $|D'|$  value indicating at most modest movement apart of the fragments. We have not obtained a similar triplet pair from DAO **3**, apparently due to its poor photolability. Formation of triplet pairs appears easiest in the most labile<sup>3</sup> DAO **1** in agreement with Symons's suggestion<sup>6</sup> that phenoxy–phenoxy radical-pair formation is most likely if decarbonylation is facile and rapid.

Overall, these ESR results are consistent with only modest movement<sup>21</sup> of each phenoxy fragment from precursor positions after photolysis of DAO's **1** and **2**, to yield the postulated radical pairs. We hope to report further aspects (e.g. temperature- and wavelength-dependent effects, single-crystal results) of this new photochemical method of radical and radical-pair generation in future work.

**Acknowledgment.** This work was supported by the Office of Naval Research and the Exxon Education Foundation. We thank Prof. Dennis Dougherty for supplying a copy of the program used by us to simulate randomly oriented triplet ESR lineshapes and Prof. Edwin Hilinski for helpful discussions concerning the use of the ZFS simulation program.

**Supplementary Material Available:** A description of our procedure for simulating zfs parameters by the McWeeny method,<sup>15,16</sup> X-ray crystallographic descriptions for **2** and **3** including crystallographic data, atomic positional and thermal parameters, bond distances and angles, molecular structure representations, and a listing of program ZFS<sup>16</sup> (32 pages); table of observed and calculated structure factors (18 pages). Ordering information is given on any current masthead page.

(16) Hilinski, E. F. Ph.D. Thesis, Yale University, 1982.

(17) Rule, M.; Matlin, A. R.; Seeger, D. E.; Hilinski, E. F.; Dougherty, D. A.; Berson, J. A. *Tetrahedron* **1982**, *38*, 787. We did not use the correction factor of 0.5 used by these workers for simulation of their zfs  $|D'/hc|$  values.

(18) Prabhanada, B. S. *J. Chem. Phys.* **1983**, *79*, 5752.

(19) In even a very simple pairwise interacting dipolar model<sup>6</sup> using experimental  $\pi$  spin densities placed right at phenoxy radical atomic sites,<sup>18</sup>  $|D'| = 122$  G.

(20) INDO calculations with doublet-unrestricted Hartree-Fock (UHF) optimized geometries and MO wavefunctions show spin density in the C=O region decreasing only ~3% upon 4-methoxy substitution.

(21) Upon prolonged photolysis of **1**, selective bleaching of the triplet spectra a and c described in this paper occurs, leaving the monoradical central peak plus what appears to be a narrower triplet spectrum with  $|D'| = 52$  G,  $|E'| \approx 0$  G, and  $g_{iso} = 2.005$ . Similar spectra are obtained from prolonged photolysis of a variety of other DAO's, consistent with phenoxy–phenoxy radical pairs having an effective distance of about 8 Å. While the nature of these triplet signal carriers is still unclear to us, they may represent interactions between phenoxy fragments produced from different DAO precursor molecules, or between fragments from a single photodecomposed DAO substantially reoriented due to photolytic lattice breakdown in an extensively irradiated crystal matrix.